finding the factor $f_a(v_x)$. Indeed as (r_0/Λ) reduces, the errors in finding c' and y do contribute to large errors in finding Q^* and Z_{max}, due to the smallness of (a/λ) and hence the detectability suffers immensely. The limit for detectability by this method appears, in a preliminary estimate, to be $(r_0/\lambda) \approx 0.12$, far lower than the limit put by Baltes and others for detection by usual intensity measurements.

The effectiveness of our method can be understood from the following argument. In the discussions on detectability, Baltes and others considered whether the $n = 0$ and the $n = 1$ peaks could be seen separately. This means they were tackling the distinguishability of two peaks whose amplitudes differ by a factor of $(a/\lambda)^2$ and which are separated by $\Delta v_x = Q$. In our extended matched filtering, once the $n = 0$ peak is filtered out we are to distinguish the two comparable peaks at $n = \pm 1$ but separated by a larger $\Delta v_x = 2Q^*$. The latter, according to the Rayleigh criterion or the Sparrow criterion[18,19], allows distinguishability of the peaks for much lower values of r_0. In the results presented here the errors are indeed tolerable, but the errors in Q^* and a reach as high as 30%, when $(r_0/\Lambda) \sim 0.065$. This communication unmistakably establishes the extended matched filtering as a promising new tool for detection of hidden periodicities, purely from intensity data. Numerical experiments choosing various sets of parameters are under way and we further plan to advance this scheme by making a statistical error analysis and issues of goodness-of-fit.

1. Beckman, P. and Spizzichino, A., *The Scattering of Electromagnetic Waves from Random Surfaces*, Pergamon Press, London, 1963.
2. Beckman, P., Scattering of light by rough surfaces. In *Progress in Optics* (ed. Wolf, E.), North Holland, 1967, vol. 6, p. 53.
3. Chatterjee, S., On the scattering of light by a periodic structure in presence of randomness. *Indian J. Phys. B*, 2000, **74**, 363–366.
4. Baltes, H. P., Fewerda, H. A., Glass, A. S. and Steinle, B., Retrieval of structural information from far zone intensity and coherence of scattered radiation. *Opt. Acta*, 1981, **28**, 11–28.
5. Baltes, H. P. and Ferwerda, H. A., Inverse problems and coherence. *IEEE Trans. Antennas Propag.*, 1981, **AP–29**, 405–406.
6. Baltes, H. P., Glass, A. S. and Jauch, K. M., Multiplexing of coherence by beam splitters. *Opt. Acta*, 1981, **28**, 873–876.
7. Baltes, H. P. and Jauch, K. M., Multiple version of the van Zittert – Zernike theorm. *J. Opt. Soc. Am.*, 1981, **71**, 1434–1439.
8. Glass, A. S. and Baltes, H. P., The significance of far zone coherence for sources or scatterers with hidden periodicity. *Opt. Acta*, 1982, **29**, 169–185.
9. Glass, A. S., Baltes, H. P. and Jauch, K. M., The detection of hidden diffractors by coherence measurements. *Proc. Soc. Photo-Opt. Instrum. Eng.*, 1982, **369**, 681–686.
10. Jauch, K. M. and Baltes, H. P., Coherence of radiation scattered by gratings covered by a diffuser. Experimental evidence. *Opt. Acta*, 1981, **28**, 1013–1015.
11. Glass, A. S., The significance of image reversal in the detection of hidden diffractors by interferometry. *Opt. Acta*, 1982, **29**, 575–583.
12. Jauch, K. M. and Baltes, H. P., Reversing wave front interferometry of radiation from a diffusively illuminated phase grating. *Opt. Lett.*, 1982, **7**, 127–129.
13. Jauch, K. M., Baltes, H. P. and Glass, A. S., Measurement of coherence of radiation from diffusively illuminated bean splitters. *Proc. Soc. Photo-Opt. Instrum. Eng.*, 1982, **369**, 687–690.
14. Dainty, J. C. and Newman, D., Detection of gratings hidden by diffusers using photon correlation techniques. *Opt. Lett.*, 1983, **8**, 608–610.
15. Chatterjee, S. and Vani, V. C., Scattering of light by periodic structure with randomness. *Bull. Astron. Soc. India*, 2002, **30**, 835–836.
16. Chatterjee, S. and Vani, V. C., On the scattering of light by a periodic structure in the presence of randomness II. On the detection of weak periodicities. *J. Mod. Opt.*, 2003, **50**, 833–845.
17. Vani, V. C. and Chatterjee, S., An extended matched filtering method to detect periodicities in a rough grating for extremely large roughness. *Bull. Astron. Soc. India*, 2003 (communicated).
18. Barakat, R., Application of apodization to increase two point resolution by the Sparrow criterion I. Coherent illumination. *J. Opt. Soc. Am.*, 1962, **52**, 276–283.
19. Barakat, R. and Levin, E., Application of apodization to increase two point resolution by the Sparrow criterion. II Incoherent illumination. *J. Opt. Soc. Am.*, 1963, **53**, 274–282.

Arabian Sea mini warm pool during May 2000

K. V. Sanilkumar*, P. V. Hareesh Kumar, Jossia Joseph and J. K. Panigrahi

Naval Physical and Oceanographic Laboratory, Thrikkakkara, Kochi 682 021, India

Anomalously warmer waters, viz. the Arabian Sea mini warm pool were reported in the southeastern Arabian Sea, which is believed to drive the onset vortex of the southwest monsoon. To understand the characteristics of this mini warm pool, an experiment was conducted on-board *INS Sagardhwani* during the middle of May 2000. Analysis of the oceanographic data revealed the existence of a mini warm pool with temperature in excess of 30.25°C along 9°N between 68 and 75.5°E during the pre-onset period of the southwest monsoon. This mini warm pool coincided with the regions of low salinity (35.2 PSU) layer and its intensity inversely correlated with the depth of the highly stable ($E > 2000 \times 10^{-8}$ m^{-1}) layer. At the core (73.5°E, 9°N) of the mini warm pool, surface temperature was 31.2°C and sea surface salinity was less than 34.6 PSU. This core was found restricted to the upper 5 m water column following the thickness of low-salinity pocket and the

*For correspondence. (e-mail: tsonpol@vsnl.com)

resulting increased vertical density stratification. This communication clearly brings out the vertical stability as an important parameter to correlate the intensity of the warm pool. With the occurrence of the southwest monsoon conditions, this mini warm pool dissipated (SST decreased to ~ 30°C). Evidences were obtained for the recirculation of low salinity Bay of Bengal water mass under the influence of a clockwise gyre in the study region.

A zone of anomalous warm water $(30.8°C)^1$ was noticed in the upper layers of the southeastern Arabian Sea prior to the onset of the southwest monsoon, which coincides with the onset vortex[2,3]. This anomalous water is named as the Arabian Sea mini warm pool. Few studies highlight the importance of this mini warm pool for the onset and rainfall variability of the southwest monsoon[2–5]. Utilizing the historic datasets, Rao and Sivakumar[3] diagnostically analysed the various factors to unravel this phenomenon. The evolving stage of this warm pool is believed to start with the formation of Laccadive High resulting from the incoming Rossby waves[6–8] during November/December. Its intensity, extent and location vary from year to year. In general, during the pre-monsoon season, due to clear skies and weak winds, heat accumulates in the upper layers of the Arabian Sea[9,10], which leads to the formation of shallow mixed layers. In addition, in the southeastern Arabian Sea, low salinity Bay of Bengal water mass was observed in the shallow mixed layer[3], which produces more stratification below the layer. Heat accumulates[11] above this highly stratified layer and leads to the formation of the mini warm pool. This mini warm pool, which is the long-lasting warmest water among the world oceanic regions[12,13], is conducive for the formation of onset vortices of the southwest monsoon[2,3]. Moreover, the higher rate of transfer of heat and water vapour due to the higher surface temperature, and its geographical extent affect the monsoon onset and rainfall over India. Onset and advance of the southwest monsoon in the Indian Ocean dissipate the mini warm pool. Despite all these important factors, exclusive experiments to observe the oceanographic conditions of the Arabian Sea mini warm pool have not been carried out so far. Hence, an experiment was conducted in the Arabian Sea during May 2000 to study the characteristics of this mini warm pool.

INS Sagardhwani made a survey along two spatial transects (along 9 and 10.5°N lat.) across the warm pool, i.e. between 67 and 76°E long. during 13–19 May 2000 (Figure 1). During this survey, temperature and salinity profiles were collected using a Mini CTD (conductivity, temperature and depth) system of SAIV, Norway (accuracy: temperature ± 0.01°C, salinity ± 0.02 PSU) at 0.5 degree interval along the transects. Surface meteorological parameters were also collected to understand the prevailing weather.

In general, pre-monsoon conditions (clear sky, atmospheric pressure > 1010 mb) prevailed east of 68.5°E along

9°N, and monsoon conditions (overcast sky, atmospheric pressure ~ 1005 mb, frequent rains) prevailed west of 68.5°E and all along 10.5°N (Figure 2). Along 9°N, sea surface temperature (SST) continuously increased towards east up to 73.5°E and decreased further towards the coast. Correspondingly, the mixed layer depth (MLD), defined as the depth at which the temperature drops by 0.2°C (ref. 14) from SST, shoaled to a minimum of 5 m around 73.5°N and deepened (> 20 m) thereafter. Along 10.5°E, SST was comparatively lower and did not exhibit any warming trend towards east (steady around 30°C) due to the onset of southwest monsoon.

The depth–space section of temperature (Figure 3 *a*) revealed temperature in excess of 30.25°C in the upper layers along 9°N, except near the coast and west of 68.5°E. On closer examination it can be seen that there is a zone of anomalous warmer waters (> 30.75°C) between 72.5 and 74°E, occupying the upper 8 m of the water column (Figure 3). At the core (73.5°E, around the Laccadive region), temperature in the upper thin layer (< 5 m) even exceeded 31.2°C. Such regions of high temperature (> 31°C) were quite unusual in other parts of the world oceans. From the core (i.e. from 73.5°E), temperature decreased towards the east and west, with a corresponding increase in MLD. The reduction in temperature towards the east was rapid (1.6°C over 220 km, i.e. from 31.2°C at 73.5°E to 29.6°C at 75.5°E), while the decrease was gradual towards the west (1.2°C over 600 km, i.e. from 31.2°C at 73.5°E to 30°C at 68°E). East of 75.5°E, the isotherms slope towards the coast suggesting coastal upwelling, resulting in low temperature (~ 29.6°C). As the southwest monsoon condition had already set in (Figure 2) along 10.5°N, temperature in the surface layers decreased by more than 1°C. The intermittent appearance of 30°C isotherms around noon coincided with the afternoon heating.

The vertical section of salinity along the 9°N track (Figure 3 *b*) indicated a layer of low salinity (< 35.2 PSU) waters in the surface layers. Thickness of this low salinity layer showed large spatial variations, with minimum thickness around 68°E (5 m). Here, the isohalines showed a bell-shaped structure indicating divergence, which was
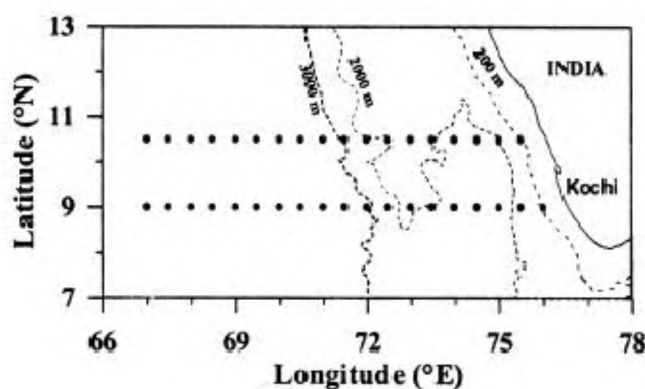

Figure 1. Locations of stations.

evident from the temperature and density structure also (Figure 3 *a* and *c*). Probably, this divergence may be due to a cyclonic eddy. Further, the thickness increased both towards the east and west. Maximum thickness (60 m) was observed around 69.5°E and then decreased gradually towards the east till it disappeared at 75°E under the influence of upwelling. On closer look, it can be seen that sea surface salinity (SSS) reached a minimum of < 34.6 PSU and appeared as intermittent pockets at a few places with varying dimensions. It is interesting to note that in the region of the warmest waters (31.2°C at 9°N, 73.5°E), thickness of the low salinity (35.2 PSU) layer approached a minimum and the SSS was also minimum (< 34.6 PSU). Similarly, when the thickness of the low salinity layer increased westwards, the SST decreased correspondingly. This observation shows that there is an inverse relation between thickness of the low salinity layer and SST along the 9°N track. However, such a relation was not observed along the 10.5°N track, which may be due to the fact that monsoon conditions had already set in this track. Moreover, the thickness of the low salinity (< 35.2 PSU) layer reduced considerably and was restricted within the 25 m water column as intermittent pockets. Corresponding to the low (34.6 PSU) SSS pockets, low density (< 21.5 sigma-*t*) waters appeared in the respective regions along both transects (Figure 3 *c*). The sigma-*t* property[15] of these low salinity pockets suggests that they originate from the Bay of Bengal, as reported in earlier studies[3,7].

In addition, presence of the Arabian Sea high salinity water mass (> 35.8 PSU, between 23 and 24 sigma-*t* surface; shaded by red colour in Figure 3 *b*) was observed as a subsurface salinity maximum all along 10.5°N and from 67 to 68°E and 72 to 75.5°E along 9°N. This subsurface salinity maximum exhibited upward displacement towards the eastern side due to upwelling.

Now, the question arises, which was the mini warm pool and what were its characteristics during this observational programme. In order to address these questions, the temperature section of both transects was compared. It is clear that during the pre-monsoon conditions, temperatures in excess of 30.25°C were present along 9°N and with the occurrence of the monsoon conditions, they disappeared from both transects. Considering this fact, a warm pool is defined in this study as the region where the waters of temperature in excess of 30.25°C appeared. It can be seen that the mini warm pool was present before the monsoon conditions set in along 9.5°N between 68 and 75.5°E, which coincided with the region of low salinity (< 35.2 PSU) layer. However, there was a disparity in the vertical extent of both the thickness of the low salinity layer and the warm pool. In the west (around 69°E), thickness of low salinity layer was 65 m whereas that of warm pool was only 40 m. But towards the east, the thickness of the low salinity layer decreased faster compared to that of the warm pool. This calls for some parameter other than the low salinity layer to correlate with the warm pool. It is also to be noted that the core of the warm pool appeared at 73.5°E, around which the vertical extent of the low salinity layer was thin and the SSS was low. The prevailing upwelling process near the coast limited the eastward extent of this warm pool.

It is known that when low salinity waters appear in thin surface layers, nonlinear combination of salinity and temperature produces more density stratification (vertical stability) just below the mixed layer and thereby inhibits mechanical mixing below the stratified layer. Consequently, during the situation of net heat gain to the sea, heat accumulates in the thin layer and SST can raise anomalously[3,11]. Therefore, as an alternate parameter to correlate with the warm pool characteristics, vertical stability (*E*)
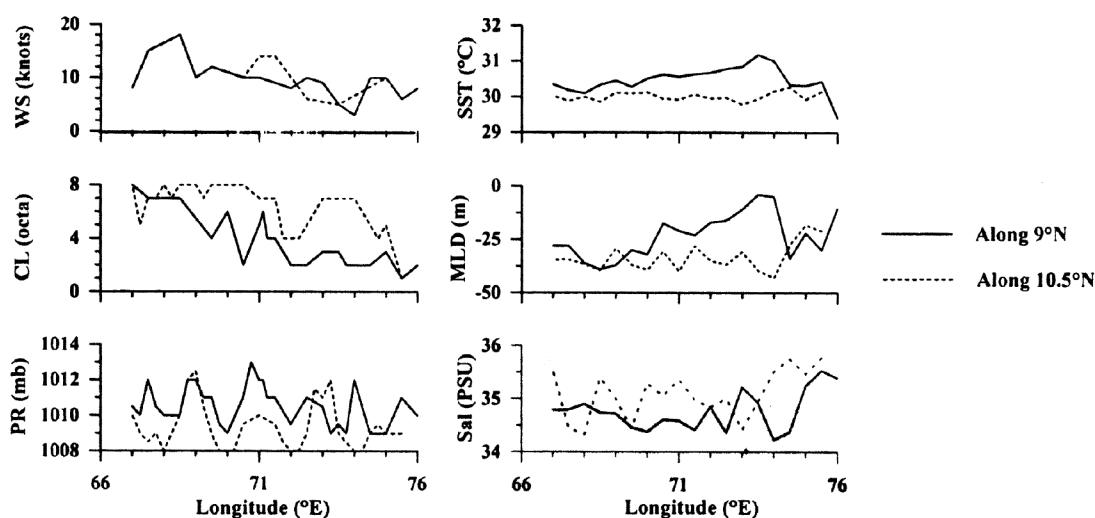

Figure 2. Distribution of wind speed (WS), cloud amount (CL), pressure (PR), sea surface temperature (SST), mixed layer depth (MLD) and salinity (Sal).

was computed[16] for each 1 m depth slab from the surface to 150 m and averaged for every 5 m slab (Figure 4) for better clarity. Highly stable layers ($E > 2000 \times 10^{-8} \, m^{-1}$, shaded by yellow in Figure 4) occurred at 40 m depth around 69°E along 9°N, where the thickness of the warm pool also matched. From this location to the west and east the depth of the stable layer decreased, which was followed by a decrease in the thickness of the warm pool also. In addition, highly stable layers appeared intermittently at the surface at few places along both transects. On verification, it was found that such stable layers were formed in the regions of thinner low salinity layers. In these cases the salinity gradient would be larger. In one such stable layer (73.5°E, 9°N), the warmest waters (31.2°C) appeared. However, this relationship between warmer waters and stable layers was seen only during the pre-monsoon period and therefore, was absent along 10.5°N where the monsoon conditions prevailed. Thus the study shows that vertical stability (stratification), which is mainly controlled by the salinity gradient near the surface, is a better parameter to correlate the warm pool characteristics.

Now it is understood that the low salinity Bay of Bengal occupies the warm pool region (Figure 3 b). Its importance on the vertical stratification and the resulting formation of the mini warm pool in southeastern Arabian Sea is also understood (Figure 4). Therefore, the mechanism of influx and trapping of this low salinity water mass needs to be examined. It is known that the North Equatorial Currents carry the Bay of Bengal water mass to the warm pool from November/December to March[3]. The thermohaline structure (Figure 3) along 9°N indicated a clockwise circulation with southward flow on the eastern side (nearer the coast). The 10.5°N track also exhibited the presence of such a clockwise gyre. However, this was weaker compared to that of the 9°N track, as evident from the comparative depths of isotherms and sigma-t surfaces between the two transects. They were at lower depths along 10.5°N due to the weaker gyre. Such a gyre can trap the incoming low salinity waters till the gyre dissipates. Recent studies observed the formation of a clockwise gyre during November/December when a Rossby wave advanced[6–8] to this region and sustained up to March/April[17]. This study provided evidences for the existence of a clockwise gyre in May also.

The study concluded that the low salinity waters and the resulting vertical density stratification in the upper layers of the southeastern Arabian Sea were conducive for the generation of the Arabian Sea mini warm pool during the pre-monsoon period. Horizontal extent of the low salinity (< 35.2 PSU) layer controlled the area of the warm pool,
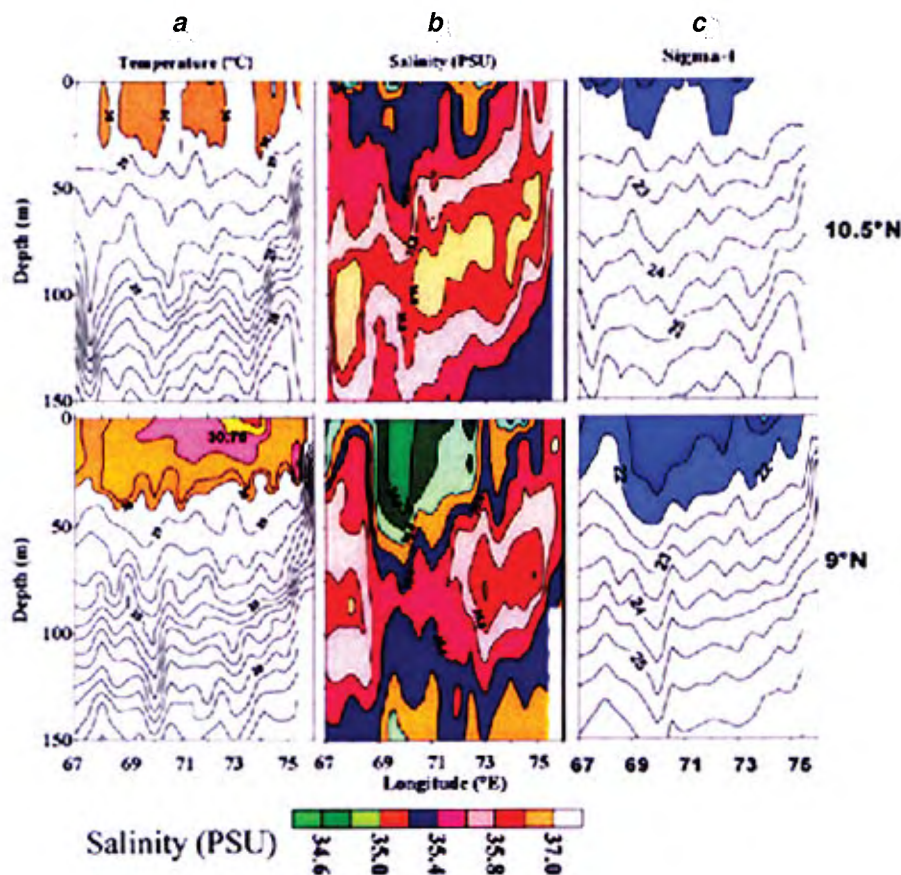

Figure 3. Depth–space sections of temperature, salinity and density along 9 and 10.5°N.
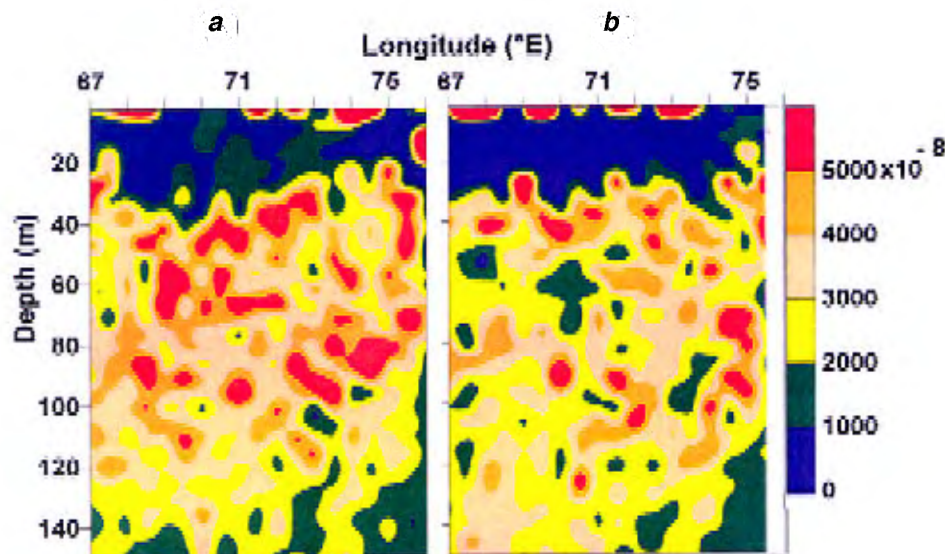
Figure 4. Vertical stability along 9°N and 10.5°N. Blue and red patches indicate weak and strong stability regions.

while the depth of the highly stratified ($E > 2000 \times 10^{-8}\,\text{m}^{-1}$) layer controlled its intensity and thickness. The warmest waters occur wherever the thinner, low salinity pockets (stratified layers) appear near the surface. The study also provides evidences for the existence of a clockwise gyre during May and the possibility of recirculation of the low salinity waters in the study region. The warm pool dissipates with the onset of the southwest monsoon.

1. Seetaramayya, P. and Master, A., Observed air–sea interface conditions and a monsoon depression during MONEX-79. *Arch. Meteorol., Geophys. Bioclimatol.*, 1984, **33**, 61–67.
2. Joseph, P. V., Warm pool over the Indian Ocean and monsoon onset. *Trop. Ocean Global Atmos. Newsl.*, 1990, **53**, 1–5.
3. Rao, R. R. and Sivakumar, R., On the possible mechanisms of the evolution of a mini-warm pool during the pre-summer monsoon season and the genesis of onset vortex in the southern Arabian Sea. *Q. J. R. Meteorol. Soc.*, 1999, **125**, 787–809.
4. Kershaw, R., Onset of the southwest monsoon and sea surface temperature anomalies in the Arabian Sea. *Nature*, 1985, **315**, 561–563.
5. Kershaw, R., The effect of a sea surface temperature anomaly in a prediction of the onset of the southwest monsoon over India. *Q. J. R. Meteorol. Soc.*, 1988, **114**, 325–345.
6. Bruce, J. G., Johnson, D. R. and Kindle, J. C., Evidence for eddy formation in the eastern Arabian Sea during the northeast monsoon. *J. Geophys. Res.*, 1994, **99**, 7651–7664.
7. Bruce, J. G., Kindle, J. C., Kantha, L. H., Kerling, J. L. and Bailey, J. F., Recent observations and modeling in the Arabian Sea Laccadive High region. *J. Geophys. Res.*, 1998, **103**, 7593–7600.
8. Shankar, D. and Shetye, S. R., On the dynamics of the Lakshadweep high and low in the southeastern Arabian Sea. *J. Geophys. Res.*, 1997, **102**, 12551–12567.
9. Hastenrath, S. and Lamb, P. J., *Climatic Atlas of the Indian Ocean. Part II: The Oceanic Heat Budget*, Wisconsin University Press, Madison, 1979, p. 17.
10. Rao, R. R., Molinari, R. L. and Festa, J. F., Evolution of the climatological near-surface thermal structure of the tropical Indian Ocean, I, Description of mean monthly mixed layer depth, sea surface temperature, surface current and surface meteorological fields. *J. Geophys. Res.*, 1989, **94**, 10801–10815.
11. Sengupta, D., Ray, P. K. and Bhat, G. S., Spring warming of the eastern Arabian Sea and Bay of Bengal from buoy data. *Geophys. Res. Lett.*, 2002, **29**, 15340–15345.
12. Shenoi, S. S. C., Shankar, D. and Shetye, S. R., On the sea surface temperature high in the Lakshadweep Sea before the onset on the southwest monsoon. *J. Geophys. Res.*, 1999, **104**, 15703–15712.
13. Department of Science and Technology, Arabian Sea Monsoon Experiment, Part II (ARMEX-II) – Warm Pool and Monsoon Onset Experiment, 2003, p. 36.
14. Camp, N. T. and Elsberry, R. L., Oceanic response to strong atmospheric forcing II. The role of one-dimensional processes. *J. Phys. Oceanogr.*, 1978, **8**, 215–224.
15. Suryanarayana, A., Murty, V. S. N. and Rao, D. P., Hydrography and circulation of the Bay of Bengal during early winter. *Deep-Sea Res.*, 1993, **40**, 205–217.
16. Pond, S. and Pickard, G. L., *Introductory Dynamic Oceanography*, Pergamon, Oxford, 1986, p. 329.
17. Han, W. and McCreary, J. P., Modeling salinity distribution in the Indian Ocean. *J. Geophys. Res.*, 2001, **106**, 859–877.
18. Cutler, A. and Swallow, J., Surface currents of the Indian Ocean (to 25 S, 100 E; compiled from historical data archived by the Meteorological Office, Bracknell, UK), Institute of Oceanographic Sciences, Technical Report 187, 1984, p. 8.